Development 138, 1121-1129 (2011) doi:10.1242/dev.058271

Pkd1l1 complexes with Pkd2 on motile cilia and functions to establish the left-right axis

Keiichiro Kamura[1], Daisuke Kobayashi[2], Yuka Uehara[1], Sumito Koshida[1], Norio Iijima[3], Akira Kudo[4], Takahiko Yokoyama[2] and Hiroyuki Takeda[1,*]

SUMMARY

The internal organs of vertebrates show distinctive left-right asymmetry. Leftward extracellular fluid flow at the node (nodal flow), which is generated by the rotational movement of node cilia, is essential for left-right patterning in the mouse and other vertebrates. However, the identity of the pathways by which nodal flow is interpreted remains controversial as the molecular sensors of this process are unknown. In the current study, we show that the medaka left-right mutant *abecobe* (*abc*) is defective for left-right asymmetric expression of *southpaw*, *lefty* and *charon*, but not for nodal flow. We identify the *abc* gene as *pkd1l1*, the expression of which is confined to Kupffer's vesicle (KV, an organ equivalent to the node). Pkd1l1 can interact and interdependently colocalize with Pkd2 at the cilia in KV. We further demonstrate that all KV cilia contain Pkd1l1 and Pkd2 and left-right dynein, and that they are motile. These results suggest that Pkd1l1 and Pkd2 form a complex that functions as the nodal flow sensor in the motile cilia of the medaka KV. We propose a new model for the role of cilia in left-right patterning in which the KV cilia have a dual function: to generate nodal flow and to interpret it through Pkd1l1-Pkd2 complexes.

KEY WORDS: Left-right asymmetry, Nodal flow, Sensor, Dual-function cilia, Left-right dynein (Lrd), Medaka

INTRODUCTION

The internal organs of vertebrates show distinctive left-right asymmetry. The establishment of left-right patterning comprises three key steps (Shiratori and Hamada, 2006). The first step is the symmetry-breaking event in the mouse embryonic node, a leftward extracellular fluid flow that is generated by the rotational movement of monocilia. The second step is the transduction of this asymmetric information to the left lateral plate mesoderm (LPM), where genes such as *Nodal* are asymmetrically expressed. In the third step, these asymmetric signals drive the morphogenesis of various asymmetric visceral organs. Ciliary motility and the resulting extracellular fluid flow (hereafter referred to as nodal flow) have also been shown to be required for left-right axis formation at the posterior notochord in rabbit, the gastrocoel roof plate in *Xenopus laevis*, and in Kupffer's vesicle (KV) in zebrafish and medaka fish, finally resulting in the asymmetrical activation of the Nodal signaling cascade in the left LPM (Essner et al., 2005; Hojo et al., 2007; Okada et al., 2005; Schweickert et al., 2007). Hence, nodal flow is highly conserved and is essential for left-right patterning in vertebrates.

However, the mechanism by which nodal flow evokes subsequent asymmetric gene cascades has proven to be elusive thus far and remains a major unanswered question in left-right patterning (Hamada, 2008; Marshall and Nonaka, 2006). There are two prevailing models. The earliest of these hypothesizes that a secreted molecule forms a concentration gradient via nodal flow, thereby triggering its receptor on the left side (Nonaka et al., 1998; Okada et al., 1999). The alternative hypothesis is the 'two-cilia model', in which the mechanical stress of the flow is sensed by a population of non-motile cilia at the periphery of the node (McGrath et al., 2003; Tabin and Vogan, 2003). To date, both models are equally plausible because the molecular sensor of nodal flow is still unknown. It remains an important task, therefore, to elucidate the molecular nature of this sensor and identify its subcellular localization.

To further elucidate the sensing mechanism of nodal flow, we have investigated the medaka left-right mutant *abecobe* (*abc*, 'inverted' in Japanese), as the underlying mutation lies downstream of nodal flow but upstream of asymmetric gene expression. We reveal that the *abc* gene is *polycystic kidney disease 1 like 1* (*pkd1l1*), which is specifically and symmetrically expressed in KV. Pkd1l1 is a member of the polycystic kidney disease (PKD) family of large membrane proteins, which are also known as the TRPP, polycystin or PC proteins. Among these factors, Pkd1 and Pkd2 were first identified as autosomal dominant PKD genes (Nauli and Zhou, 2004). These two proteins act together in the primary cilia of the renal epithelium and form a channel complex. In this structure, Pkd1, which has a large extracellular domain, is thought to mechanically sense urinary flows, whereas Pkd2 mediates Ca^{2+} influx as a channel (Nauli et al., 2003; Nauli and Zhou, 2004). Pkd2 is also known to be essential for left-right axis formation as it is localized in mouse node cilia (McGrath et al., 2003), and *Pkd2* knockout mice show organ laterality defects (Pennekamp et al., 2002). By contrast, *Pkd1* knockout mice exhibit normal left-right determination and Pkd1 is not found in mouse node cilia (Karcher et al., 2005). Hence, the co-factor for Pkd2 during left-right patterning remains unknown and the identity of the mechanism underlying Pkd2-mediated left-right patterning has been somewhat controversial (Hirokawa et al., 2006; Karcher et al., 2005; Shiratori and Hamada, 2006).

[1]Department of Biological Sciences, Graduate School of Science, University of Tokyo, Hongo, Bunkyo-ku, Tokyo 113-0033, Japan. [2]Department of Anatomy and Developmental Biology, Graduate School of Medical Science, Kyoto Prefectural University of Medicine, 465 Kaiji-cho, Kyoto 602-8566, Japan. [3]Department of Anatomy and Neurobiology, Nippon Medical School, 1-1-5 Sendagi, Bunkyo-ku, Tokyo 113-8602, Japan. [4]Department of Biological Information, Tokyo Institute of Technology, Nagatsuta, Midori-ku, Yokohama 226-8501, Japan.

*Author for correspondence (htakeda@biol.s.u-tokyo.ac.jp)

Accepted 17 December 2010

In this paper, our biochemical and immunohistochemical studies demonstrate that Pkd1l1 is the elusive partner of Pkd2 in KV. Furthermore, we show that all cilia in KV are motile and contain Pkd1l1-Pkd2 complexes. Thus, we propose a new working model for the role of KV cilia in which they have a dual function: both to generate nodal flow and to sense it through Pkd1l1-Pkd2 complexes.

MATERIALS AND METHODS

Fish strains and mapping

We used the medaka (*Oryzias latipes*) inbred strain Cab as a wild-type strain. *abc*^{aA12} was isolated from our N-ethyl-N-nitrosourea (ENU)-mediated mutant screening as previously described (Miyake et al., 2008), and *abc*^{def} was isolated spontaneously from the Cab strain. Mapping of the *abc*^{aA12} locus was carried out as previously described (Kimura et al., 2004; Miyake et al., 2008). *abc*^{aA12} and *abc*^{def} show no observable phenotypic differences. Unless otherwise noted, we used the *abc*^{aA12} allele as the *abc* mutant in these experiments. Embryos were obtained from natural crosses of homozygotes.

Whole-mount in situ hybridization

In situ hybridization analyses were performed as previously described (Hojo et al., 2007). The cDNAs used as the templates for the probes were as follows: *southpaw* and *lefty* (kindly provided by Dr H. Hashimoto, Nagoya University, Japan); *charon* (Hojo et al., 2007); and *pkd1l1*, *pkd1* and *pkd2* isolated from the Cab strain by RT-PCR using the following primers (5′ to 3′): *pkd1l1*, TACACCCTCCTGCGCAGCCAAA and GCTCATGGATGCTCTCGAATG; *pkd1*, TGGCCATCTCCTCACTGCTGATG and GAGGGTGCTGGTGTGAATGGGA; and *pkd2*, GATGAACGCCAGCACTCATTGG and TCCATGCCCTCCAGCTTCAC.

RT-PCR

RT-PCR analysis of *pkd1l1* was performed using total RNA from adult tissues and 6-somite stage medaka embryos. cDNA libraries were generated using the SuperScript First-Strand Synthesis System for RT-PCR (Invitrogen). The primers 5′-GTGTGCGGGACATTTCACAGTCA-3′ and 5′-GCTCACTAAGCAGAGTCACACTCGAA-3′ were used to amplify a 247 bp fragment of *pkd1l1*.

Observation of nodal flow and KV cilia movement

Observations of nodal flow were performed as previously described (Hojo et al., 2007) at the rate of 10 frames per second (fps). The whole KV cilia movement was captured as previously described (Omran et al., 2008) at ~100 fps and played back at 30 fps. Peripheral KV cilia movement was captured using a 63× water-immersion lens on a Leica TCS SP5 at the rate of 14 fps for normal embryos or 3.6 fps for Arl13b-GFP-expressing embryos. *Arl13b-GFP* mRNA was injected for visualizing monocilia (Borovina et al., 2010) at 415 ng/μl.

Morpholino knockdown and mRNA rescue

The morpholino antisense oligonucleotides (MOs; Gene Tools) used in this study were as follows (5′ to 3′): pkd1l1-tm2, AGAAACAACATCTGTTAGAGAAATG; pkd1l1-I7E8, CCCGTGCTGCACAGAGAACACATTT; pkd1l1-Met, CGAGAAGATCCACAGACAGAACATG; pkd2-ex3, GACAGATTTGCACCTTCCAGAAATC; and lrd-exon2/intron2, TGATTTTTAGGCTTACCGTTTGTCC (Hojo et al., 2007). mRNAs of *pkd1l1* were synthesized as reported previously (Yokoi et al., 2007). MOs or mRNAs were injected into 1- to 2-cell stage medaka embryos at 60 μM (pkd1l1-tm2), 600 μM (pkd2-ex3), 300 μM (lrd-exon2/intron2) or 300 ng/μl (*pkd1l1* mRNA).

Mammalian cell expression

Fragments encoding the N-terminus of Pkd1l1 (M1-N1911) or the C-terminus of Pkd1l1 (L1912-N2742) were inserted into the pCS2+MT vector to generate constructs that produce N-terminal Myc-tagged proteins. A Flag tag was inserted at the C-terminus of the Pkd2 open reading frame in the pCS2p+ vector. We transiently infected HEK293T cells with these various expression constructs for Pkd1l1 and Pkd2 using FuGENE HD Transfection Reagent (Roche). At 24-36 hours after transfection, the cells were used for immunoprecipitation assays. We used empty pCS2+MT or pCS2p+ vectors for the mock transfections.

Immunoprecipitation

Cell pellets were resuspended in lysis buffer [20 mM sodium phosphate, 150 mM sodium chloride, 10% glycerol, 1 mM EDTA, 0.5% Triton X-100, pH 7.2, and Complete Protease Inhibitor Cocktail (Roche)], incubated at 4°C for 2 hours, and then centrifuged at 10,000 ***g*** at 4°C for 15 minutes. The cleared lysate was incubated with c-Myc monoclonal antibody-agarose beads (Clontech) or anti-Flag M2 affinity gel (Sigma) at 4°C overnight to immunoprecipitate Myc-tagged or Flag-tagged samples, respectively. We then washed the immunoprecipitate three times with PBS and eluted with Laemmli buffer. The eluted products and an equal volume of whole-cell lysates were subjected to polyacrylamide gel electrophoresis (5% and 7.5% acrylamide for Pkd1l1 and Pkd2, respectively) and western blot analysis. Monoclonal antibody against c-Myc (9e10, Biomol) and monoclonal antibody against Flag (M2, Sigma) were used as primary antibodies at 1:7000 and 1:3000 dilution, respectively. Signals were detected with ExactaCruz E (Santa Cruz), and then developed using standard western blot protocols (ECL, Amersham).

Antibody generation

Polyclonal rabbit anti-Pkd1l1 [amino acids 1251-1500 (N-terminus) or 2550-2742 (C-terminus)] and anti-Lrd [amino acids 987-1355 (DNAH9-1) or 2011-2307 (DNAH9-2)] antibodies were raised by immunization of rabbits with bacterially expressed His-tagged truncated proteins. Zebrafish *lrdr* (*dnah9*) and medaka *lrd* (*dnah9*) are functionally equivalent to mouse *Lrd* (*Dnahc11*) (Essner et al., 2005; Essner et al., 2002; Hojo et al., 2007).

Immunofluorescence

Embryos were fixed by rinsing with 80:20 methanol:DMSO, blocked in 2% BSA/PBSDT (10% DMSO/0.2% Triton X-100/PBS) and incubated with primary antibodies in 2% BSA/PBSDT overnight at 4°C: Pkd1l1 and Lrd at 1:50; acetylated α-tubulin 6-11B-1 (T6793, Sigma) at 1:400; and Pkd2 [SC-10377 (E-20) and SC-47734 (YCE2), Santa Cruz] at 1:100. After washing in PBSDT, embryos were incubated with Alexa 488 or 555 (Molecular Probes) or Cy5 (Chemicon) conjugated secondary antibodies at 1:400. Washed embryos were cleared in 50% glycerol/PBS and photographed on a LSM710 confocal fluorescence microscope (Zeiss). Three-dimensional reconstruction was performed using maximum intensity projection with ZEN 2009 LE software (Zeiss).

Accession numbers

Nucleotide sequence data reported here are available at the DDBJ/EMBL/GenBank databases under the following accession numbers: medaka *pkd1l1* gene, AB573426; medaka *pkd2* gene, AB573427.

RESULTS

The *abecobe* mutant demonstrates abnormal left-right patterning but normal nodal flow

The *abecobe* (*abc*^{aA12}) medaka mutant was isolated in our recent ENU-driven screen for mutants with defects in embryonic development and organogenesis. *abc* is a recessive mutant defective in left-right axis determination. We first examined the position of the heart, liver and gall bladder in *abc* embryos at 5 days post-fertilization (dpf). In wild-type medaka embryos, the ventricle of the heart loops towards the right and the atrium towards the left (Fig. 1A), while the liver and the gall bladder become positioned to the left of the midline (Fig. 1C). A reversal in the direction of heart looping was observed in 5 of 737 wild-type embryos (0.68%), whereas only 1 embryo (0.14%) showed a reversal in the placement of the liver (Table 1). By contrast, reversal in the position of the heart (Fig. 1B) and the liver (Fig. 1D) was seen in 48.5% and 43.0% of *abc* embryos, respectively (Table 1), but no other defects were evident in the gross morphology,

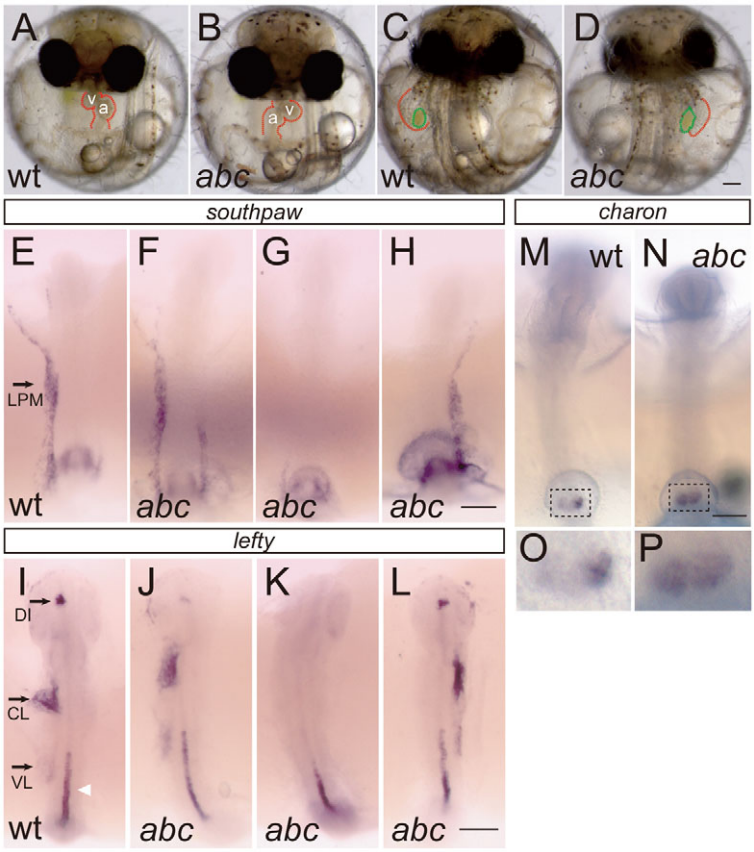

Fig. 1. Phenotype of medaka *abecobe* mutants. (**A-D**) Frontal views of the heart (A,B) and dorsal views of the liver (red) and gall bladder (green) (C,D) in medaka embryos at 5 dpf. (**E-P**) Dorsal views of (E-H) *southpaw* (8-somite stage), (I-L) *lefty* (11-somite stage) and (M-P) *charon* (9-somite stage) expression. The white arrowhead (I) indicates the notochord. (O,P) Higher magnification views of Kupffer's vesicle (KV; dashed box in M,N). wt, wild type; a, atrium; v, ventricle; LPM, lateral plate mesoderm; DI, diencephalon; CL, cardiac LPM; VL, visceral LPM. Scale bars: 100 μm.

survival or reproduction characteristics of these mutants. We thus conclude that the *abc* mutant shows a randomized left-right organ placement.

To better define the exact step in left-right patterning affected in *abc*, we examined expression of the asymmetrically expressed genes *nodal*, *lefty* and *charon*. In wild-type medaka, expression of the nodal gene *southpaw* and of a downstream target, *lefty*, is restricted to the left LPM during early somitogenesis, prior to asymmetric localization of the organs (Fig. 1E,I) (Soroldoni et al., 2007). However, the *abc* mutants displayed randomized *southpaw* expression in the LPM (Table 2), which was left sided (Fig. 1F), right sided (Fig. 1H), bilateral or absent (Fig. 1G). *lefty*, which is normally expressed in the left cardiac LPM (n=16/16), also showed left-sided (n=3/20, Fig. 1J), right-sided (n=3/20, Fig. 1L), bilateral (n=6/20) or absent (n=8/20, Fig. 1K) expression in *abc* mutants. Charon is a member of the Cerberus/DAN family of proteins and negatively regulates *southpaw* expression in the right LPM in medaka and zebrafish (Hashimoto et al., 2004; Hojo et al., 2007). Medaka *charon* is asymmetrically expressed in the KV epithelium, with more intense expression on the right than the left side (Fig. 1M,O). This asymmetry of expression is regulated by the nodal flow in KV (Hojo et al., 2007) and is thus likely to be the earliest known event at the molecular level in medaka development. The expression of *charon* in *abc* embryos was symmetrical (Fig. 1N,P), although these expression levels were variable i.e. upregulated in some embryos and downregulated in the others. These results indicate that *abc* acts upstream of asymmetric gene expression.

We then examined nodal flow in KV, an essential step in left-right axis determination in medaka and zebrafish and similar to the case in mouse (Essner et al., 2005; Hojo et al., 2007; Okada et al., 2005). For this, we injected particles of vermeil India ink into KV. The particle movement revealed a coherent directional nodal flow in KV, not only in wild-type but also in *abc* embryos (see Movies 1 and 2 in the supplementary material), indicating normally functioning KV cilia. Furthermore, no differences were observed between wild-type and *abc* embryos in the number and length of

Table 1. Defects in heart and liver asymmetry in *abc* mutant embryos

		Heart		Liver	
Genotype	n	Correct (%)	Reversed (%)	Correct (%)	Reversed (%)
Wild type	737	99.3	0.7	99.9	0.1
abc^{aA12}	507	51.5	48.5	57.0	43.0
abc^{def}	267	56.6	43.4	55.8	44.2
pkd1l1 mRNA rescue	82	86.6	13.4	90.2	9.8
pkd1l1 MO	68	91.2	8.8	97.1	2.9
pkd2 MO	66	57.6	42.4	47.0	53.0

The heart loop direction and the position of the liver were scored at 5 dpf.

Table 2. Alterations in *southpaw* expression in *abc* mutant embryos

Genotype	*n*	Left (%)	Right (%)	Bilateral (%)	Absent (%)
Wild type	39	100	0	0	0
abc^{aA12}	47	30	11	17	43
abc^{def}	22	41	27	14	18

Expression in the lateral plate mesoderm was scored at the 8-somite stage.

cilia (data not shown; see Fig. 4C,F) or in the movement of cilia per se (see Movies 3 and 4 in the supplementary material). Taken together, we conclude that *abc* functions immediately downstream of nodal flow.

The medaka *abc* gene is *pkd1l1*

To identify the defective gene in the *abc* mutant we carried out positional cloning and narrowed down the *abc*^{aA12} locus to a 109 kb region in linkage group 20, which harbors six open reading frames (Fig. 2A). One likely candidate for *abc*^{aA12} was the *pkd1l1* gene, which we hypothesized might encode the elusive partner of Pkd2. The medaka *pkd1l1* transcript is 8226 nt in length, comprises 53 exons and encodes a 2742 amino acid protein that is the ortholog of human PKD1L1 (Yuasa et al., 2002). Pkd1l1 is a member of the PKD family of proteins that contain two Ig-like PKD domains in addition to an REJ, GPS, LH2/PLAT, coiled-coil and 11 putative transmembrane domains (Fig. 2B). Sequence comparisons between *abc*^{aA12} and wild-type embryos identified a nonsense mutation in *pkd1l1* that is predicted to generate a truncated protein consisting of only the N-terminal 1911 residues.

To verify that *pkd1l1* is indeed responsible for the *abc* phenotype, wild-type *pkd1l1* mRNA was injected into homozygous *abc* embryos and was found to efficiently rescue the *abc* phenotype (Table 1). Antisense morpholino oligonucleotide (MO) knockdown of *pkd1l1* proved less effective for technical reasons (see Fig. S1 in the supplementary material); the phenotype was, however, partially but significantly phenocopied when an MO directed against an exon-intron boundary in the second transmembrane domain (pkd1l1-tm2) was injected (Table 1). Further, we isolated a second mutation, *abc*^{def} (def, deficient 3′ end), from a wild-type population; this mutant encodes an aberrant *pkd1l1* transcript harboring extra sequences at the 3′ end (see Fig. S2 in the supplementary material) and sequence comparison revealed a transposon insertion. Such insertions have been observed in the scaleless medaka mutant *rs-3* (Kondo et al., 2001) and the PKD medaka mutant *pc* (Hashimoto et al., 2009). Collectively, we concluded that medaka *pkd1l1* is the gene responsible for the *abc* mutant.

Medaka *pkd1l1* is expressed in KV

To determine the expression pattern of *pkd1l1*, we performed whole-mount in situ hybridization of epiboly and early somite stage embryos. Expression was first detected at the onset of KV formation at the 100% epiboly stage (data not shown) and was strictly confined to the KV epithelium (Fig. 3A,C). This expression peaked at the 0- to 3-somite stage and progressively decreased as KV enlarged, eventually disappearing by the 9-somite stage (when KV is at its largest; data not shown). By contrast, *pkd1l1* transcripts were undetectable in the *abc* KV (Fig. 3B,D), probably owing to nonsense-mediated mRNA decay (NMD) (Wittkopp et al., 2009). We additionally analyzed *pkd1l1* expression in adult tissues by RT-PCR and found positive signals in multiple tissues, including the testis and heart (see Fig. S3 in the supplementary material). It has been reported previously that human *PKD1L1* is expressed in these tissues (Yuasa et al., 2002), but the expression profile in early embryos had not been determined. The exclusive expression of *pkd1l1* in KV during the early somite stages implies a crucial role for *pkd1l1* in KV.

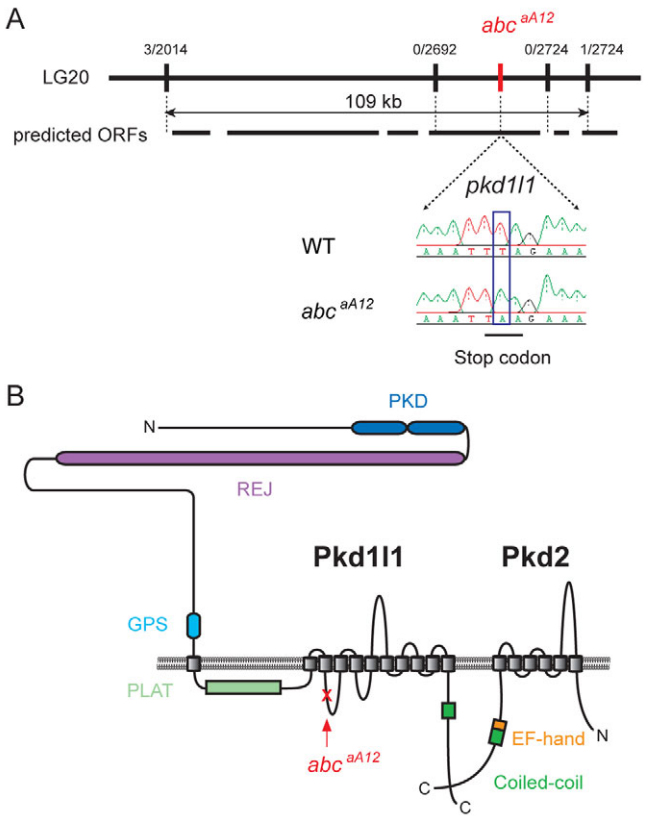

Fig. 2. Identification and structure of medaka *abecobe* (*pkd1l1*). (**A**) Positional cloning of the *abc* mutation in linkage group (LG) 20. The number of recombinants at each marker is shown. The nature of the mutation in *pkd1l1* that is responsible for *abc*^{aA12} is illustrated beneath. (**B**) Predicted membrane topology of Pkd1l1 and Pkd2. ORF, open reading frame.

Medaka *pkd2* is also involved in left-right axis formation

Since Pkd1 may not be involved in left-right axis formation in mouse (Karcher et al., 2005), we speculated that Pkd1l1 could be the partner of Pkd2 in the node (KV). We therefore examined the expression patterns of *pkd1* and *pkd2* in early somite-stage medaka embryos by in situ hybridization. As expected, *pkd1* showed ubiquitous expression at extremely low levels in both wild-type and *abc* embryos (Fig. 3E,F), whereas *pkd2* was found to be ubiquitously but highly expressed (Fig. 3H,I). *pkd2* transcripts were apparent in the KV epithelium in wild type as well as in *abc*. The essential role of *pkd2* in left-right axis formation has been reported in mouse and zebrafish (Bisgrove et al., 2005; Pennekamp et al., 2002; Schottenfeld et al., 2007), and we therefore examined its role in medaka. When a *pkd2* MO designed to block splicing was injected, the resulting embryos exhibited left-right patterning abnormalities that were comparable to those of *abc* mutants (Table 1). This indicates that medaka *pkd2* also plays a role in left-right axis formation.

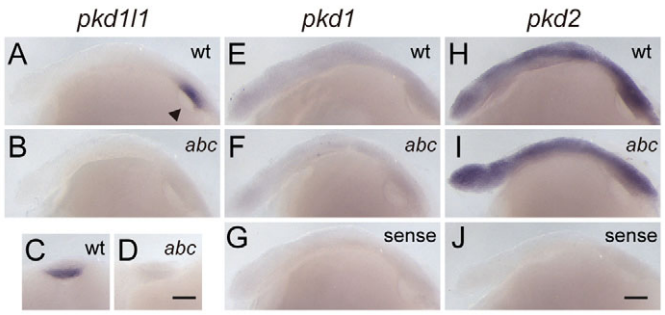

Fig. 3. Expression of medaka *pkd1l1*, *pkd1* and *pkd2*. (**A-J**) Lateral (A,B,E-J) and caudal (C,D) views of 3-somite stage wild-type (wt) and *abc* embryos subject to in situ hybridization for *pkd1l1* (A-D), *pkd1* (E-G) and *pkd2* (H-J). Sense hybridizations (G,J) are negative controls. Arrowhead (A) indicates KV. Scale bars: 100 μm.

Pkd1l1 interacts with Pkd2

Because PKD1 and PKD2 were previously shown to interact in the kidney and thereby function as a fluid-flow sensor (Hanaoka et al., 2000; Nauli et al., 2003), we hypothesized that Pkd1l1 and Pkd2 would operate in this way in KV. This was first assessed by co-immunoprecipitation assays. Mammalian expression vectors encoding the Myc-tagged C-terminal half of Pkd1l1 including the predicted coiled-coil domain (Myc-Pkd1l1 C-terminus) and Flag-tagged Pkd2 (Pkd2-Flag) were transfected into HEK293T cells. After the cell extracts were precipitated with anti-Flag antibodies, proteins were eluted and analyzed by western blotting. The Myc-Pkd1l1 C-terminus protein was detected as a band of ~106 kDa (Fig. 4A, lane 3). By contrast, we could not detect any co-precipitation product when the Myc-Pkd1l1 N-terminus (i.e. the abc^{aA12} mutant form of Pkd1l1) was used (data not shown). Likewise, when Myc-Pkd1l1 C-terminus was precipitated, Pkd2-Flag was specifically co-purified (Fig. 4A, lane 7).

In the kidney epithelium, Pkd1 is required for the localization of Pkd2 to cilia (Nauli et al., 2003). To test whether this is also the case for Pkd1l1 in KV, we analyzed the localization of Pkd2 in the presence or absence of Pkd1l1. Whole-mount immunofluorescence staining revealed the localization of Pkd2 to monocilia in KV at early somite stages (E-20; Fig. 4B). Labeling with antibodies against acetylated α-tubulin revealed that Pkd2 is normally uniformly distributed in the KV monocilia (Fig. 4C,D). By contrast, *abc* embryos showed a complete absence of ciliary staining by anti-Pkd2 antibodies (Fig. 4E,G), although the distribution and length of KV monocilia appeared normal (Fig. 4F). Similar results were obtained using another independent Pkd2 antibody (YCE2). A previous study demonstrated that native or transfected human PKD2 accumulates in the endoplasmic reticulum (ER) (Cai et al., 1999). We found this to be the case for medaka Pkd2, as in transfected HEK cells this signal was observed in a fine reticular cytoplasmic and perinuclear pattern consistent with expression in the ER (data not shown). Immunofluorescence analysis of the KV epithelium further showed faint staining for Pkd2 in the cytoplasm (Fig. 4H), which was completely abolished in the *pkd2* morphant (Fig. 4J). However, the cytoplasmic staining pattern for Pkd2 was unchanged in *abc* embryos (Fig. 4I). These observations suggest that the interaction between Pkd1l1 and Pkd2 is required for the ciliary localization of Pkd2 in KV.

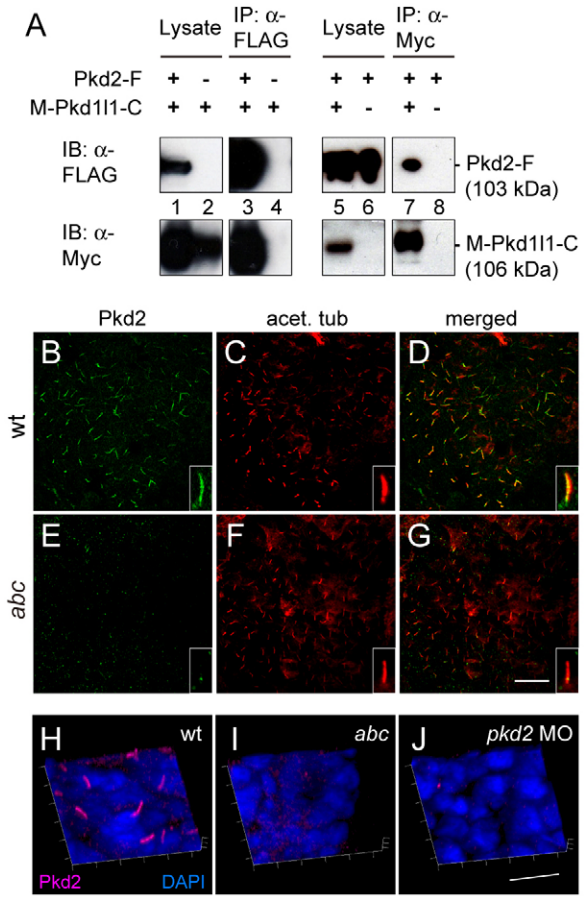

Fig. 4. Interaction between Pkd1l1 and Pkd2. (**A**) Co-immunoprecipitation of Pkd1l1 and Pkd2. HEK293T cells were co-transfected with the Myc-Pkd1l1 C-terminus (M-Pkd1l1-C) and/or Pkd2-Flag (Pkd2-F) constructs. –, mock transfection; IB, immunoblot; IP, immunoprecipitation. (**B-G**) Localization of Pkd2 (green) to KV monocilia. Cilia (acet. tub, acetylated α-tubulin, red) in KV of wild-type and *abc* mutant embryos at the 4-somite stage are shown. Insets show higher magnifications of cilia. (**H-J**) Three-dimensional images of Pkd2 localization to KV monocilia and in the cytoplasm. Scale bars: 20 μm in G; 10 μm in J.

All KV cilia contain Pkd1l1-Pkd2 complexes

A previous study demonstrated that the mouse node contains two types of monocilia – motile and immotile – and proposed a two-cilia model (McGrath et al., 2003; Tabin and Vogan, 2003). These two types of cilia are distinguished by the presence or absence of the axonemal dynein heavy chain known as left-right dynein (Lrd). Centrally located monocilia contain Lrd and generate nodal flow, whereas peripheral nodal cilia lack Lrd but contain Pkd2 and thus function as a flow sensor in the mouse. Based on this model and our finding of Pkd1l1 as the partner of Pkd2, we expected that Pkd1l1 proteins would be located on immotile peripheral KV cilia. We therefore examined the subcellular localization of medaka Pkd1l1 using an antibody raised against the C-terminus of the protein. The *abc* mutations create a premature stop codon, resulting in the expression of truncated forms of Pkd1l1 that are not recognized by the antibody used. In wild-type KV, as expected, Pkd1l1 staining colocalized with that of acetylated α-tubulin. Surprisingly, however, this staining was uniformly found in all cilia (Fig. 5A; n=26). There were no significant spatial variations in the Pkd1l1 staining intensity

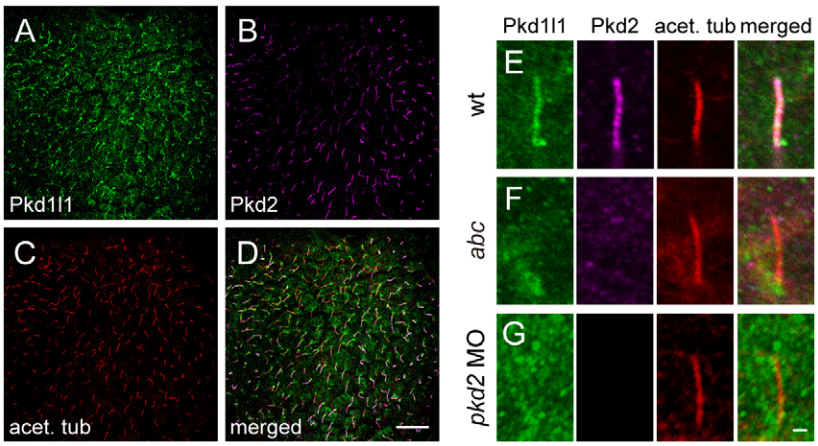

Fig. 5. Colocalization of Pkd1l1 and Pkd2 at KV monocilia. (**A-D**) Cilia (acet. tub, acetylated α-tubulin, red) in KV of a wild-type medaka embryo at the 4-somite stage stained for Pkd1l1 (green) and Pkd2 (magenta). D is a merge of all three stainings. (**E-G**) High-magnification view of a KV monocilium stained as in A-D in wild type, *abc* and a *pkd2* morphant. Scale bars: 20 μm in D; 1 μm in G.

across KV or along the entire cilium (Fig. 5E). We found a very similar labeling pattern with another antibody raised against the N-terminus of medaka Pkd1l1 (data not shown). In *abc* KV, however, no staining was evident in the cilia (Fig. 5F; *n*=9). In the control experiments, no positive staining was observed with pre-immune serum or in the absence of primary antibody (data not shown). To further examine the relationship between Pkd1l1 and Pkd2 in the KV monocilia, double immunofluorescence staining was performed using the Pkd1l1 and Pkd2 antibodies. These proteins were found to colocalize in all KV cilia along their entire length (Fig. 5A-E). Furthermore, Pkd1l1 failed to localize to KV cilia in *pkd2* morphants (Fig. 5G; *n*=2), indicating that Pkd1l1 and Pkd2 are interdependent for their localization to the KV cilia. These observations suggest that all KV cilia contain Pkd1l1-Pkd2 complexes.

All cilia in KV contain left-right dynein

We then examined whether the two-cilia model of two subsets of cilia (centrally motile and peripherally immotile) holds true in the medaka KV. To determine the distribution of Lrd among medaka KV cilia, we generated an antibody against medaka Lrd (DNAH9-2). Interestingly, immunostaining showed that the medaka Lrd is present in all KV cilia along their entire length (Fig. 6A-D; *n*=10). No populations of Lrd-negative monocilia were observed on either the central or peripheral KV epithelium. This was also the case for *abc* embryos (Fig. 6E; *n*=4; data not shown). The specificity of the antibody was confirmed by the absence of Lrd immunoreactivity in wild-type embryos injected with MOs targeting an exon-intron boundary of medaka *lrd* (Fig. 6F; *n*=4). We also found a very similar labeling pattern with another antibody raised against medaka Lrd (DNAH9-1) (data not shown). Moreover, no positive staining was observed with pre-immune serum or in the absence of the primary antibody (data not shown). From these results, we conclude that the medaka KV does not contain a distinct subset of immotile cilia. Consistent with this, nearly all cilia, including peripheral cilia, in wild-type and *abc* KV were found to be motile when observed by live imaging (see Movie 5 in the supplementary material). This was confirmed using wild-type and *abc* embryos that express Arl13b-GFP (see Movie 6 in the supplementary material) specifically localized to monocilia (Borovina et al., 2010).

DISCUSSION

A possible role of Pkd1l1 in sensing nodal flow

In our current study, we identified *pkd1l1* as the gene mutated in the medaka left-right mutant *abc*. *Pkd1l1* was first cloned from human and mouse (Yuasa et al., 2002) and belongs to the Pkd1 family, which encodes 11-transmembrane proteins. Recently, the *Pkd1l1* knockout mouse was identified by high-throughput screening (Vogel et al., 2010) and found to exhibit organ laterality defects similar to those of *abc* medaka mutants. However, despite a brief phenotypic description, the expression and function of Pkd1l1 remained unknown until studies from our laboratory and by Field et al. (Field et al., 2011). The gene name *polycystic kidney disease 1 like 1* indicates the sequence similarity to *pkd1* (Yuasa et al., 2002). In humans, mutations in *PKD1* or *PKD2* result in autosomal dominant polycystic kidney disease (ADPKD); these two proteins are localized to primary cilia in the renal epithelium (Yoder et al., 2002). PKD2 is known to form a functional ion-conducting channel, whereas PKD1, with its large extracellular domain, is thought to sense the bending of a primary cilium induced by fluid flow in the renal tubule, thus functioning as a mechanosensor (Nauli et al., 2003).

In addition to renal cyst formation, *Pkd2* knockout mice show left-right patterning defects (Pennekamp et al., 2002), which is also the case for zebrafish *pkd2* morphants and mutants (Bisgrove et al., 2005; Schottenfeld et al., 2007). Pkd2 is localized to monocilia in the mouse node and has been reported to mediate a left-sided calcium signal (McGrath et al., 2003). In our present study, we demonstrate that medaka *pkd2* is also involved in left-right patterning and that Pkd2 localizes to the monocilia in KV, indicating a conserved role in left-right patterning. Hence, Pkd2 functions in both the kidney and node. Interestingly, however, Pkd1 was shown in previous studies not to be a functional partner of Pkd2 in the mouse node in terms of left-right axis formation: *Pkd1* knockout mice do not display laterality defects and no ciliary localization of Pkd1 was detected in the mouse node (Karcher et al., 2005). This is consistent with our current results showing that *pkd1* is almost undetectable in the medaka KV. Hence, the counterpart of Pkd1 in left-right patterning has thus far remained unknown. We propose here that Pkd1l1 is a strong candidate because of its KV-restricted expression and left-right-specific mutant phenotype.

Pkd1l1 and Pkd2 function coordinately in KV

Our co-immunoprecipitation assays revealed that the C-terminal half of Pkd1l1 is required for the heteromeric interaction between Pkd1l1 and Pkd2. Consistently, PKD1 and PKD2 are known to interact with each other through the coiled-coil domains in their C-terminal cytoplasmic tails and thereby form a functional channel (Hanaoka et al., 2000; Qian et al., 1997; Tsiokas et al., 1997). Since Pkd1l1 also contains a putative

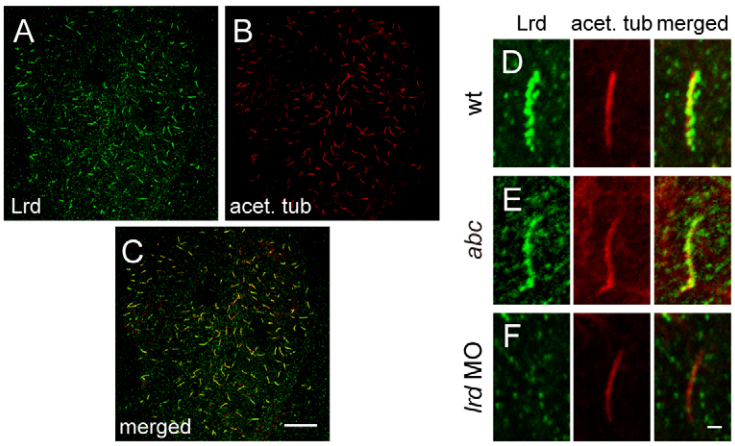

Fig. 6. Localization of Lrd to KV monocilia. (**A-C**) Cilia (acet. tub, acetylated α-tubulin, red) in KV of a wild-type medaka embryo at the 4-somite stage showing localization of Lrd (green). (**D-F**) High-magnification view of a KV monocilium stained as in A-C in wild type, *abc* and a *lrd* morphant. Scale bars: 20 μm in C; 1 μm in F.

coiled-coil domain in its C-terminal cytoplasmic tail, a similar interaction between Pkd1l1 and Pkd2 could mediate the formation of a functional channel. By contrast, the N-terminal half of Pkd1l1, which is equivalent to the *abc*^{aA12} form of Pkd1l1, does not bind to Pkd2 and therefore no functional complex should be formed in the *abc*^{aA12} mutant medaka embryos. The interaction between Pkd1l1 and Pkd2 was also confirmed in vivo by examining their subcellular localization. Pkd1l1 and Pkd2 colocalize to KV cilia, but Pkd2 fails to do so in the absence of Pkd1l1 and vice versa. Similar results were reported previously for Pkd1 and Pkd2, in which the co-distribution of these proteins at the cilia was observed in wild-type mouse kidney epithelial cells, but Pkd2 signal was not detected in *Pkd1* mutant cells (Nauli et al., 2003). Thus, complex formation could be a prerequisite for the proper trafficking of these proteins to the cilia.

All cilia in the medaka KV are motile

One of the most important findings of our present study is that all monocilia in the medaka KV are motile. In the mouse, Lrd has been shown to localize to a centrally located subset of node monocilia (motile cilia), whereas Lrd-negative monocilia (immotile cilia) have been observed in the peripheral node (McGrath et al., 2003). Our current findings, however, indicate that all cilia in the medaka KV are positive for Lrd and rotate to generate nodal flow. For technical reasons, we cannot absolutely exclude the presence of immotile cilia, but they would not be peripherally located as a distinct subpopulation in the medaka KV. This discrepancy in ciliary type and pattern between mouse and medaka could reflect structural differences in the node (KV) between these two species. In the mouse node, two distinct regions can be discerned: pit cells, which are columnar and monociliated, and, surrounding them, crown cells, which are squamous and less often ciliated (Bellomo et al., 1996; Lee and Anderson, 2008). By contrast, no such morphological differences are observed within fish KV. Indeed, *charon*, a immediate target of nodal flow (Hojo et al., 2007), is widely expressed in the KV epithelial cell (Fig. 1O,P), but the mouse ortholog cerberus-like 2 (*Cerl2*; also known as *Dand5* – Mouse Genome Informatics) and the *Xenopus* ortholog *coco* are expressed at the periphery of the node (gastrocoel roof plate in *Xenopus*) (Marques et al., 2004; Schweickert et al., 2010). More importantly, the fact that all cilia are motile in KV has led us to reconsider the two-cilia model for vertebrates as discussed below.

How do KV cilia interpret nodal flow?

Directional nodal flow should be translated into asymmetric gene expression in the node/KV epithelium. Our present results suggest that Pkd1l1 and Pkd2 form a sensor complex that is present in all KV cilia, and that all KV cilia are motile. Hence, in fish, the generators and sensors of nodal flow are not segregated, suggesting that KV cilia could have both functions (Fig. 7); this is apparently inconsistent with the two-cilia model. Recently, there has been a growing awareness that motile cilia are capable of mechanosensation and/or chemosensation (for a review, see Bloodgood, 2010). For example, motile cilia in the respiratory tract and oviduct are known to adjust ciliary beat frequency in response to viscosity changes in the extracellular fluid (Bloodgood, 2010), and human airway epithelial cells sense bitter compounds through T2R receptors localized on motile cilia (Shah et al., 2009); the latter is a good example of chemosensation by motile cilia. Which type of sensing does Pkd1l1 perform? Pkd1 and Pkd1l1 both have a large extracellular domain extending from the multiple transmembrane domain, but these domains show few similarities (Yuasa et al., 2002). This suggests that Pkd1l1 senses something different from the mechanical forces sensed by Pkd1 (Nauli et al., 2003). Indeed, other Pkd1 homologs function in a variety of organs and receive a variety of signals (Ong and Harris, 2005), although the precise mechanisms are still largely unknown. Pkd1l3 and Pkd2l1 are coexpressed in a subset of taste receptor cells and have been implicated in sour taste reception (Ishimaru et al., 2006). PKDREJ (receptor for egg jelly) is localized on the mouse sperm head and has been suggested to respond to the zona pellucida matrix to trigger the acrosome reaction (Butscheid et al., 2006;

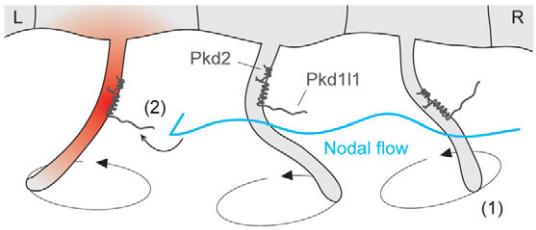

Fig. 7. Model of the mechanism of nodal flow in KV. KV cilia have a dual function: (1) rotating to generate nodal flow; and (2) sensing nodal flow mechanically or chemically through Pkd1l1-Pkd2 complexes. L, left; R, right.

Hughes et al., 1999). In *Caenorhabditis elegans*, the Pkd1 ortholog *lov-1* and the Pkd2 ortholog are expressed in adult male sensory neurons and are required for male mating behavior, suggesting their function as sensory receptors (Barr et al., 2001; Barr and Sternberg, 1999). Since it appears that rotating KV cilia cannot mechanically sense the direction of nodal flow, which is an essential parameter for interpretation of asymmetric liquid flow (Cartwright et al., 2004), we currently hypothesize that Pkd1l1 on motile cilia functions in chemosensation rather than in mechanosensation.

Based on the studies of Field and colleagues (Field et al., 2011), the requirement for Pkd1l1-Pkd2 complexes during left-right patterning is conserved between medaka and mouse. Pkd1l1-Pkd2 complexes are likely to operate via a general molecular mechanism of nodal flow sensing among vertebrates. However, there are two questions that need to be addressed. The first is the phenotypic difference between mice and teleosts when the function of Pkd1l1/Pkd2 is defective: *Nodal* expression in the LPM is largely lost in mice (Field et al., 2011; Pennekamp et al., 2002), whereas *Nodal* expression tends to be randomized in zebrafish (Bisgrove et al., 2005; Schottenfeld et al., 2007) and medaka (Fig. 1F-H). This suggests that there are some differences in the mechanism of robust asymmetric *Nodal* expression in the left LPM. Second, whether dual-function cilia are conserved among species remains a fascinating question. At present, the localization of Pkd1l1-Pkd2 complexes is unknown in any species other than medaka. Although it is conceivable that Pkd1l1 proteins localize only on peripheral immotile cilia in the mouse node, it is more plausible that mouse Pkd1l1 proteins also localize on all node monocilia, as observed in medaka, because mouse Pkd2 proteins are found in all node monocilia (McGrath et al., 2003). In any case, future studies on the localization of Pkd1l1 protein in various species will add further important insights into the sensing mechanisms that underlie nodal flow.

Conclusions

We have shown that Pkd1l1 is the long-sought functional partner of Pkd2 in left-right patterning and that Pkd1l1 and Pkd2 colocalize on motile cilia in the medaka KV. Furthermore, we propose a new model in which the generation and interpretation of nodal flow are both achieved by a single population of motile cilia in fish KV. Further studies of Pkd1l1 function will clarify the sensing mechanism for nodal flow and whether dual-function cilia are conserved among species.

Acknowledgements

We thank Dominic P. Norris and colleagues for helpful discussion and for sharing data prior to publication; Brian Ciruna for providing the Arl13b-GFP expression construct; Yasuko Ozawa for excellent fish care; Shinya Ooki for his contribution to the initial mapping of *abc*^{a12}; Akiko Takahashi for experimental support; and Atsuko Shimada for discussion and comments on the manuscript. This work was supported in part by Grants-in-Aid for Scientific Research Priority Area Genome Science and Scientific Research and for Scientific Research on Innovative Areas, Global COE Program from the Ministry of Education, Culture, Sports, Science and Technology of Japan. K.K. was a recipient of a Fellowship of the Japan Society for the Promotion of Science for Junior Scientists.

Competing interests statement

The authors declare no competing financial interests.

Supplementary material

Supplementary material for this article is available at
http://dev.biologists.org/lookup/suppl/doi:10.1242/dev.058271/-/DC1

References

Barr, M. M. and Sternberg, P. W. (1999). A polycystic kidney-disease gene homologue required for male mating behaviour in C. elegans. *Nature* **401**, 386-389.

Barr, M. M., DeModena, J., Braun, D., Nguyen, C. Q., Hall, D. H. and Sternberg, P. W. (2001). The Caenorhabditis elegans autosomal dominant polycystic kidney disease gene homologs lov-1 and pkd-2 act in the same pathway. *Curr. Biol.* **11**, 1341-1346.

Bellomo, D., Lander, A., Harragan, I. and Brown, N. A. (1996). Cell proliferation in mammalian gastrulation: the ventral node and notochord are relatively quiescent. *Dev. Dyn.* **205**, 471-485.

Bisgrove, B. W., Snarr, B. S., Emrazian, A. and Yost, H. J. (2005). Polaris and Polycystin-2 in dorsal forerunner cells and Kupffer's vesicle are required for specification of the zebrafish left-right axis. *Dev. Biol.* **287**, 274-288.

Bloodgood, R. A. (2010). Sensory reception is an attribute of both primary cilia and motile cilia. *J. Cell Sci.* **123**, 505-509.

Borovina, A., Superina, S., Voskas, D. and Ciruna, B. (2010). Vangl2 directs the posterior tilting and asymmetric localization of motile primary cilia. *Nat. Cell Biol.* **12**, 407-412.

Butscheid, Y., Chubanov, V., Steger, K., Meyer, D., Dietrich, A. and Gudermann, T. (2006). Polycystic kidney disease and receptor for egg jelly is a plasma membrane protein of mouse sperm head. *Mol. Reprod. Dev.* **73**, 350-360.

Cai, Y., Maeda, Y., Cedzich, A., Torres, V. E., Wu, G., Hayashi, T., Mochizuki, T., Park, J. H., Witzgall, R. and Somlo, S. (1999). Identification and characterization of polycystin-2, the PKD2 gene product. *J. Biol. Chem.* **274**, 28557-28565.

Cartwright, J. H., Piro, O. and Tuval, I. (2004). Fluid-dynamical basis of the embryonic development of left-right asymmetry in vertebrates. *Proc. Natl. Acad. Sci. USA* **101**, 7234-7239.

Essner, J. J., Vogan, K. J., Wagner, M. K., Tabin, C. J., Yost, H. J. and Brueckner, M. (2002). Conserved function for embryonic nodal cilia. *Nature* **418**, 37-38.

Essner, J. J., Amack, J. D., Nyholm, M. K., Harris, E. B. and Yost, H. J. (2005). Kupffer's vesicle is a ciliated organ of asymmetry in the zebrafish embryo that initiates left-right development of the brain, heart and gut. *Development* **132**, 1247-1260.

Field, S., Riley, K.-R., Grimes, D. T., Hilton, H., Simon, M., Powles-Glover, N., Siggers, P., Bogani, D., Greenfield, A. and Norris, D. P. (2011). Pdk1l1 establishes left-right asymmetry and physically interacts with Pkd2. *Development* **138**, 1131-1142.

Hamada, H. (2008). Breakthroughs and future challenges in left-right patterning. *Dev. Growth Differ.* **50 Suppl. 1**, S71-S78.

Hanaoka, K., Qian, F., Boletta, A., Bhunia, A. K., Piontek, K., Tsiokas, L., Sukhatme, V. P., Guggino, W. B. and Germino, G. G. (2000). Co-assembly of polycystin-1 and -2 produces unique cation-permeable currents. *Nature* **408**, 990-994.

Hashimoto, H., Rebagliati, M., Ahmad, N., Muraoka, O., Kurokawa, T., Hibi, M. and Suzuki, T. (2004). The Cerberus/Dan-family protein Charon is a negative regulator of Nodal signaling during left-right patterning in zebrafish. *Development* **131**, 1741-1753.

Hashimoto, H., Miyamoto, R., Watanabe, N., Shiba, D., Ozato, K., Inoue, C., Kubo, Y., Koga, A., Jindo, T., Narita, T. et al. (2009). Polycystic kidney disease in the medaka (Oryzias latipes) pc mutant caused by a mutation in the Gli-Similar3 (glis3) gene. *PLoS ONE* **4**, e6299.

Hirokawa, N., Tanaka, Y., Okada, Y. and Takeda, S. (2006). Nodal flow and the generation of left-right asymmetry. *Cell* **125**, 33-45.

Hojo, M., Takashima, S., Kobayashi, D., Sumeragi, A., Shimada, A., Tsukahara, T., Yokoi, H., Narita, T., Jindo, T., Kage, T. et al. (2007). Right-elevated expression of charon is regulated by fluid flow in medaka Kupffer's vesicle. *Dev. Growth Differ.* **49**, 395-405.

Hughes, J., Ward, C. J., Aspinwall, R., Butler, R. and Harris, P. C. (1999). Identification of a human homologue of the sea urchin receptor for egg jelly: a polycystic kidney disease-like protein. *Hum. Mol. Genet.* **8**, 543-549.

Ishimaru, Y., Inada, H., Kubota, M., Zhuang, H., Tominaga, M. and Matsunami, H. (2006). Transient receptor potential family members PKD1L3 and PKD2L1 form a candidate sour taste receptor. *Proc. Natl. Acad. Sci. USA* **103**, 12569-12574.

Karcher, C., Fischer, A., Schweickert, A., Bitzer, E., Horie, S., Witzgall, R. and Blum, M. (2005). Lack of a laterality phenotype in Pkd1 knock-out embryos correlates with absence of polycystin-1 in nodal cilia. *Differentiation* **73**, 425-432.

Kimura, T., Jindo, T., Narita, T., Naruse, K., Kobayashi, D., Shin, I. T., Kitagawa, T., Sakaguchi, T., Mitani, H., Shima, A. et al. (2004). Large-scale isolation of ESTs from medaka embryos and its application to medaka developmental genetics. *Mech. Dev.* **121**, 915-932.

Kondo, S., Kuwahara, Y., Kondo, M., Naruse, K., Mitani, H., Wakamatsu, Y., Ozato, K., Asakawa, S., Shimizu, N. and Shima, A. (2001). The medaka rs-3 locus required for scale development encodes ectodysplasin-A receptor. *Curr. Biol.* **11**, 1202-1206.

Lee, J. D. and Anderson, K. V. (2008). Morphogenesis of the node and notochord: the cellular basis for the establishment and maintenance of left-right asymmetry in the mouse. *Dev. Dyn.* **237**, 3464-3476.

Marques, S., Borges, A. C., Silva, A. C., Freitas, S., Cordenonsi, M. and Belo, J. A. (2004). The activity of the Nodal antagonist Cerl-2 in the mouse node is required for correct L/R body axis. *Genes Dev.* **18**, 2342-2347.
Marshall, W. F. and Nonaka, S. (2006). Cilia: tuning in to the cell's antenna. *Curr. Biol.* **16**, R604-R614.
McGrath, J., Somlo, S., Makova, S., Tian, X. and Brueckner, M. (2003). Two populations of node monocilia initiate left-right asymmetry in the mouse. *Cell* **114**, 61-73.
Miyake, A., Higashijima, S., Kobayashi, D., Narita, T., Jindo, T., Setiamarga, D. H., Ohisa, S., Orihara, N., Hibiya, K., Konno, S. et al. (2008). Mutation in the abcb7 gene causes abnormal iron and fatty acid metabolism in developing medaka fish. *Dev. Growth Differ.* **50**, 703-716.
Nauli, S. M. and Zhou, J. (2004). Polycystins and mechanosensation in renal and nodal cilia. *BioEssays* **26**, 844-856.
Nauli, S. M., Alenghat, F. J., Luo, Y., Williams, E., Vassilev, P., Li, X., Elia, A. E., Lu, W., Brown, E. M., Quinn, S. J. et al. (2003). Polycystins 1 and 2 mediate mechanosensation in the primary cilium of kidney cells. *Nat. Genet.* **33**, 129-137.
Nonaka, S., Tanaka, Y., Okada, Y., Takeda, S., Harada, A., Kanai, Y., Kido, M. and Hirokawa, N. (1998). Randomization of left-right asymmetry due to loss of nodal cilia generating leftward flow of extraembryonic fluid in mice lacking KIF3B motor protein. *Cell* **95**, 829-837.
Okada, Y., Nonaka, S., Tanaka, Y., Saijoh, Y., Hamada, H. and Hirokawa, N. (1999). Abnormal nodal flow precedes situs inversus in iv and inv mice. *Mol. Cell* **4**, 459-468.
Okada, Y., Takeda, S., Tanaka, Y., Belmonte, J. C. and Hirokawa, N. (2005). Mechanism of nodal flow: a conserved symmetry breaking event in left-right axis determination. *Cell* **121**, 633-644.
Omran, H., Kobayashi, D., Olbrich, H., Tsukahara, T., Loges, N. T., Hagiwara, H., Zhang, Q., Leblond, G., O'Toole, E., Hara, C. et al. (2008). Ktu/PF13 is required for cytoplasmic pre-assembly of axonemal dyneins. *Nature* **456**, 611-616.
Ong, A. C. and Harris, P. C. (2005). Molecular pathogenesis of ADPKD: the polycystin complex gets complex. *Kidney Int.* **67**, 1234-1247.
Pennekamp, P., Karcher, C., Fischer, A., Schweickert, A., Skryabin, B., Horst, J., Blum, M. and Dworniczak, B. (2002). The ion channel polycystin-2 is required for left-right axis determination in mice. *Curr. Biol.* **12**, 938-943.
Qian, F., Germino, F. J., Cai, Y., Zhang, X., Somlo, S. and Germino, G. G. (1997). PKD1 interacts with PKD2 through a probable coiled-coil domain. *Nat. Genet.* **16**, 179-183.
Schottenfeld, J., Sullivan-Brown, J. and Burdine, R. D. (2007). Zebrafish curly up encodes a Pkd2 ortholog that restricts left-side-specific expression of southpaw. *Development* **134**, 1605-1615.
Schweickert, A., Weber, T., Beyer, T., Vick, P., Bogusch, S., Feistel, K. and Blum, M. (2007). Cilia-driven leftward flow determines laterality in Xenopus. *Curr. Biol.* **17**, 60-66.
Schweickert, A., Vick, P., Getwan, M., Weber, T., Schneider, I., Eberhardt, M., Beyer, T., Pachur, A. and Blum, M. (2010). The nodal inhibitor Coco is a critical target of leftward flow in Xenopus. *Curr. Biol.* **20**, 738-743.
Shah, A. S., Ben-Shahar, Y., Moninger, T. O., Kline, J. N. and Welsh, M. J. (2009). Motile cilia of human airway epithelia are chemosensory. *Science* **325**, 1131-1134.
Shiratori, H. and Hamada, H. (2006). The left-right axis in the mouse: from origin to morphology. *Development* **133**, 2095-2104.
Soroldoni, D., Bajoghli, B., Aghaallaei, N. and Czerny, T. (2007). Dynamic expression pattern of Nodal-related genes during left-right development in medaka. *Gene Expr. Patterns* **7**, 93-101.
Tabin, C. J. and Vogan, K. J. (2003). A two-cilia model for vertebrate left-right axis specification. *Genes Dev.* **17**, 1-6.
Tsiokas, L., Kim, E., Arnould, T., Sukhatme, V. P. and Walz, G. (1997). Homo- and heterodimeric interactions between the gene products of PKD1 and PKD2. *Proc. Natl. Acad. Sci. USA* **94**, 6965-6970.
Vogel, P., Read, R., Hansen, G. M., Freay, L. C., Zambrowicz, B. P. and Sands, A. T. (2010). Situs inversus in Dpcd/Poll$^{-/-}$, Nme7$^{-/-}$, and Pkd1l1$^{-/-}$ mice. *Vet. Pathol.* **47**, 120-131.
Wittkopp, N., Huntzinger, E., Weiler, C., Sauliere, J., Schmidt, S., Sonawane, M. and Izaurralde, E. (2009). Nonsense-mediated mRNA decay effectors are essential for zebrafish embryonic development and survival. *Mol. Cell. Biol.* **29**, 3517-3528.
Yoder, B. K., Hou, X. and Guay-Woodford, L. M. (2002). The polycystic kidney disease proteins, polycystin-1, polycystin-2, polaris, and cystin, are co-localized in renal cilia. *J. Am. Soc. Nephrol.* **13**, 2508-2516.
Yokoi, H., Shimada, A., Carl, M., Takashima, S., Kobayashi, D., Narita, T., Jindo, T., Kimura, T., Kitagawa, T., Kage, T. et al. (2007). Mutant analyses reveal different functions of fgfr1 in medaka and zebrafish despite conserved ligand-receptor relationships. *Dev. Biol.* **304**, 326-337.
Yuasa, T., Venugopal, B., Weremowicz, S., Morton, C. C., Guo, L. and Zhou, J. (2002). The sequence, expression, and chromosomal localization of a novel polycystic kidney disease 1-like gene, PKD1L1, in human. *Genomics* **79**, 376-386.